Tuning the Intramolecular Charge Transfer of Alkynylpyrenes: Effect on Photophysical Properties and Its Application in Design of OFF–ON Fluorescent Thiol Probes

ARTICLE *in* THE JOURNAL OF ORGANIC CHEMISTRY · JUNE 2009

Impact Factor: 4.72 · DOI: 10.1021/jo900588e · Source: PubMed

6 AUTHORS, INCLUDING:

Jun Yang
Dalian University of Technology
21 PUBLICATIONS **237** CITATIONS

SEE PROFILE

JOC Article

Tuning the Intramolecular Charge Transfer of Alkynylpyrenes: Effect on Photophysical Properties and Its Application in Design of OFF−ON Fluorescent Thiol Probes

Shaomin Ji,[†] Jun Yang,[‡] Qing Yang,[‡] Shasha Liu,[§] Maodu Chen,[§] and Jianzhang Zhao*,[†]

State Key Laboratory of Fine Chemicals, School of Chemical Engineering, Department of Bioscience and Biotechnology, School of Biological and Environmental Science and Technology, and School of Physics and Optoelectronic Technology, Dalian University of Technology, 158 Zhongshan Road, Dalian 116012, P.R. China

zhaojzh@dlut.edu.cn

Received March 18, 2009

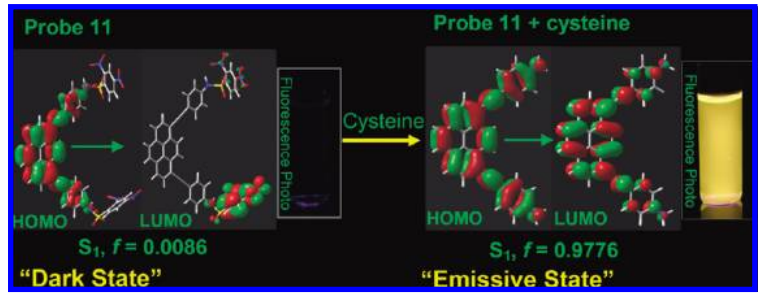

Green and yellow-emitting 1,6- and 1,8-bis(phenylethynyl) pyrenes (dyes **7**, **8**, **9**, and **10**) with different intramolecular charge transfer (ICT) feature were synthesized and the effect of ICT on the photophysical properties of these derivatives were studied by UV−vis absorption spectra, fluorescence emission spectra, and DFT/TDDFT calculations. For the dyes with electron-pushing group (e.g., -dimethylamino, dye **8** and dye **10**), structureless and solvent polarity-sensitive fluorescence emission spectra were observed. Conversely, dye with electron-withdrawing group (e.g., −CN, dye **7**) shows structured and solvent polarity-independent emission spectra. OFF−ON fluorescent thiol probes **11** and **12** with 2,4-dinitrobenzenesulfonyl protected ethynylpyrene fluorophore were designed based on DFT/TDDFT calculations, which predicts dark state (S_1) for these thiol probes (e.g., oscillator strength $f = 0.0086$ for $S_1 \leftarrow S_0$ transition of the probe **11**). This dark state is induced by the ICT effect with ethynylated pyrene fluorophore as electron donor and 2,4-dinitrobenzenesulfonyl unit as electron acceptor. Cleavage of the 2,4-dinitrobenzenesulfonyl unit by thiol releases the free fluorophore, for which the lowest-lying excited state S_1 is no longer a dark state, but an emissive state ($f = 0.9776$ for $S_1 \leftarrow S_0$ transition). These theoretical predictions on the photophysical properties of the molecular probes were fully proved by experimental results. Our results demonstrated that the fluorescence OFF−ON switching of this kind of thiol probe is due to the termination of the ICT effect (which quenches the emission, by a dark S_1 state) by cleavage of the 2,4-dinitrobenzenesulfonyl unit (as acceptor of ICT effect) with thiols, not the re-establishment of the D-π-A feature of the fluorophore. These investigation on the pyrene derived green-emitting fluorophores and the DFT/TDDFT calculation aided probe design suggest that future application of these results may prove useful toward the rational design of fluorophores or fluorescent probes with predetermined photophysical properties.

Introduction

Fluorescent molecular probes are in great interest due to their versatile applications in chemical, environmental and biological science.[1] Fluorophores are the fundamental building blocks of fluorescent probes. Concerning this aspect, the critical properties of the fluorophores are excitation/emission wavelength, Stokes shifts, fluorescent quantum yields (especially in aqueous solution), solvent polarity sensitivity of the emission, etc. Besides appropriate fluorophores, proper sensing mechanism is also essential for successful probe design. Popular fluorescence sensing mechanisms include intramolecular charge transfer (ICT), photoinduced electron transfer (PET) and metal chelation

[†] School of Chemical Engineering.
[‡] School of Biological and Environmental Science and Technology.
[§] School of Physics and Optoelectronic Technology.

10.1021/jo900588e CCC: $40.75 © 2009 American Chemical Society
Published on Web 05/21/2009

enhanced fluorescent, etc.[1] Currently, design of fluorescence probes is usually based on trial and error method, not a rational approach, for example guided by theoretical calculations on the photophysical properties (e.g., with density functional theory calculations, DFT).[2] This lack of rationale in the design makes it difficult to prepare probes with predetermined photophysical properties.

Pyrene is a versatile fluorophore, which shows featured excimer/monomer emission and exceptionally long fluorescence lifetime (τ is up to 400 ns in deaerated solution, compared to τ < 10 ns for most organic fluorophores).[1a,b,3−6] However, pyrene suffers from short excitation/emission wavelength (emission is less than 450 nm, in UV or blue range) and high oxygen sensitivity of its emission (emission is dramatically quenched in the presence of oxygen, O_2).[1a,b] The blue emission makes it difficult to be used for in vivo fluorescence bioimaging because the background-fluorescence of the biological sample will exert significant interference. Moreover, the significant quenching effect of O_2 on the emission of pyrene may diminish the probe's sensitivity on molecular sensing.[1a,b] Therefore, preparation of pyrene derivatives with emission at longer wavelength and oxygen-independent emission is of great interest.[6] Recently, pyrene derivatives with extended π-conjugation system and red-shifted emission have been reported.[3,6−9] Preliminary application of these new pyrene derivatives as fluorescent probes is promising.[6] Inspired by all these works and the recent elegant design of thiol probes with new sensing mechanism (thiol induced deprotection of 2,4-dinitrobenzenesulfonyl protected fluorophore),[10−12] a sensing strategy which shows excellent immunity to interference from nitrogen and oxygen nuleophiles, we set out to synthesis new pyrene-based fluorophores and design new thiol probes based on these new fluorophores, which show fluorescence at 560 nm. Furthermore, we investigated the sensing mechanism of this new kind of thiol probes from a point of view of theoretical chemistry. Better understanding of the sensing mechanism is achieved.

Herein we prepared 1,6- and 1,8-bis(phenylethynyl) pyrenes (dyes **7**−**10**) via Sonogashira coupling reaction. The new derivatives give emission centered at 560 nm, which is red-shifted by ca. 200 nm compared to pyrene. The photophysical properties of the derivatives were found to be dependent on the intramolecular charge transfer (ICT) feature. On the basis of theoretical calculations, we designed new alkynylpyrene-based fluorescent thiol probes. The calculations predict lowest-lying dark excited states S_1 for the thiol probes **11** and **12**, which make the probes nonfluorescent. With cleavage of the 2,4-dinitrobenzenesulfonyl unit by thiol, thus elimination of the ICT effect (2,4-dinitrobenzenesulfonyl unit as the electron acceptor), the fluorophore is released, for which the TDDFT calculation shows an emissive S_1 state and as a result, the deprotected probe becomes fluorescent. These theoretical predictions on the fluorescence OFF−ON property of the probe were fully proved by experimental results. Our finding demonstrate that the fluorescence OFF−ON effect of the probe in the presence of thiol is due to the elimination of the ICT effect (quenching effect, with 2,4-dinitrobenzenesulfonyl unit as the electron acceptor), not the recovery of the D-π-A feature of the fluorophore.[11] Our investigation on the photophysical properties of the alkynylpyrenes and the DFT/TDDFT calculation aided rational probe design approach will be helpful for future development of organic fluorophores and molecular probes with predetermined photophysical properties.

Results and Discussion

Synthesis. Synthesis of the pyrene derivatives are outlined in Scheme 1. First pyrene was iodized, but the resulted 1,6-diioide and 1,8-diioide pyrene were difficult to be isolated from each other. Therefore, a further alkynylation was carried out to prepare a mixture of **3** and **4**, which can be easily purified with column chromatography to give 1,6-diethynyl and 1,8-diethynylpyrene.[13] Electron withdrawing as well as electron pushing groups were appended on the phenylethynyl pyrenes to study the ICT effect on the photophysical property of the derivatives. We noticed the solubility of these compounds in normal organic solvents is poor.

Guided by DFT and time-dependent DFT (TDDFT) calculations for the dyes,[2] we designed fluorescent thiol probes **11** and **12**, with phenylethynyl pyrene unit as the fluorophore and 2,4-dinitrobenzenesulfonyl as the thiol reactive group (Scheme 1). Amino group appended phenylethynyl pyrene was reacted with 2,4-dinitrobenzenesulfonyl chloride, with 2,6-dimethylpyridine

(1) (a) Lakowicz, J. R. *Principles of Fluorescence Spectroscopy*, 2nd ed.; Kluwer Academic/Plenum Publishers: New York, 1999. (b) Valeur, B. *Molecular Fluorescence: Principles and Applications*; Wiley-VCH Verlag: GmbH, 2001. (c) Parson, W. W. *Modern Optical Spectroscopy: With Examples from Biophysics and Biochemistry*; Springer-Verlag: Berlin Heidelberg, 2007. (d) James, T. D.; Shinkai, S. *Top. Curr. Chem.* **2002**, *218*, 159. (e) Bell, T. W.; Hext, N. M. *Chem. Soc. Rev.* **2004**, *33*, 589. (f) Lavigne, J. J.; Anslyn, E. V. *Angew. Chem., Int. Ed.* **2001**, *40*, 3118. (g) Davis, A. P.; Wareham, R. S. *Angew. Chem., Int. Ed.* **1999**, *38*, 2978. (h) Mohr, G. J. *Chem.—Eur. J.* **2004**, *10*, 1082. (i) Oshovsky, G. V.; Reinhoudt, D. N.; Verboom, W. *Angew. Chem., Int. Ed.* **2007**, *46*, 2366. (j) Stibor, I.; Zlatušková, P. *Top. Curr. Chem.* **2005**, *255*, 31. (k) Pu, L. *Chem. Rev.* **2004**, *104*, 1687. (l) Martínez-Máñez, R.; Sancenón, F. *J. Fluoresc.* **2005**, *15*, 267. (m) Gale, P. A. *Coord. Chem. Rev.* **2003**, *240*, 191. (n) de Silva, A. P.; Fox, D. B.; Huxley, A. J. M.; McClenaghan, N. D.; Roiron, J. *Coord. Chem. Rev.* **1999**, *185−186*, 297. (o) Kang, S. O.; Begum, R. A.; Bowman-James, K. *Angew. Chem., Int. Ed.* **2006**, *45*, 7882. (p) Filby, M. H.; Steed, J. W. *Coord. Chem. Rev.* **2006**, *250*, 3200. (q) dos Santos, C. M. G.; McCabe, T.; Watson, G. W.; Kruger, P. E.; Gunnlaugsson, T. *J. Org. Chem.* **2008**, *73*, 9235. (r) Liu, W.-X.; Jiang, Y.-B. *J. Org. Chem.* **2008**, *73*, 1124. (s) Wolf, C.; Xuefeng, M. *J. Am. Chem. Soc.* **2003**, *125*, 10651. (t) Galbraith, E.; Fyles, T. M.; Marken, F.; Davidson, M. G.; James, T. D. *Inorg. Chem.* **2008**, *47*, 6236. (u) Benniston, A. C.; Chapman, G. M.; Harriman, A.; Rostron, S. A. *Inorg. Chem.* **2005**, *44*, 4029. (v) Alamiry, M. A. H.; Benniston, A. C.; Copley, G.; Elliott, K. J.; Harriman, A.; Stewart, B.; Zhi, Y.-G. *Chem. Mater.* **2008**, *20*, 4024.

(2) (a) Cody, J.; Mandal, S.; Yang, L.; Fahrni, C. J. *J. Am. Chem. Soc.* **2008**, *130*, 13023. (b) McCarroll, M. E.; Shi, Y.; Harris, S.; Puli, S.; Kimaru, I.; Xu, R.; Wang, L.; Dyer, D. J. *J. Phys. Chem. B.* **2006**, *110*, 22991. (c) Sunahara, H.; Urano, Y.; Kojima, H.; Nagano, T. *J. Am. Chem. Soc.* **2007**, *129*, 5597. (d) Han, F.; Chi, L.; Liang, X.; Ji, S.; Liu, S.; Zhou, F.; Wu, Y.; Han, K.; Zhao, J.; James, T. D. *J. Org. Chem.* **2009**, *74*, 1333. (e) Potter, R. G.; Hughes Thomas, S. *J. Org. Chem.* **2008**, *73*, 2995. (f) FrischM. J.; *Gaussian 03, revision B.05*; Gaussian Inc.: Pittsburgh PA, 2003.

(3) Kim, H. M.; Lee, Y. O.; Lim, C. S.; Kim, J. S.; Cho, B. R. *J. Org. Chem.* **2008**, *73*, 5127.

(4) (a) Kim, H. J.; Hong, J.; Hong, A.; Ham, S.; Lee, J. H.; Kim, J. S. *Org. Lett.* **2008**, *10*, 1963. (b) Benniston, A. C.; Harriman, A.; Llarena, I.; Sams, C. A. *Chem. Mater.* **2007**, *19*, 1931.

(5) (a) Yang, S.-W.; Elangovan, A.; Hwang, K.-C.; Ho, T.-I. *J. Phys. Chem. B* **2005**, *109*, 16628. (b) Benniston, A. C.; Harriman, A.; Lawrie, D. J.; Mayeux, A. *Phys. Chem. Chem. Phys.* **2004**, *6*, 51. (c) Benniston, A. C.; Harriman, A.; Lawrie, D. J.; Mayeux, A.; Rafferty, K.; Russell, O. D. *Dalton Trans.* **2003**, 4762. (d) Leroy, S.; Soujanya, T.; Fages, F. *Tetrahedron Lett.* **1998**, *39*, 1179.

(6) Maeda, H.; Maeda, T.; Mizuno, K.; Fujimoto, K.; Shimizu, H.; Inouye, M. *Chem.—Eur. J.* **2006**, *12*, 824.

(7) Shimizu, H.; Fujimoto, K.; Furusyo, M.; Maeda, H.; Nanai, Y.; Mizuno, K.; Inouye, M. *J. Org. Chem.* **2007**, *72*, 1530.

(8) (a) Venkataramana, G.; Sankararaman, S. *Eur. J. Org. Chem.* **2005**, 4162. (b) Dioubankova, N. N.; Malakhov, A. D.; Shenkarev, Z. O.; Korshun, V. A. *Tetrahedron* **2004**, *60*, 4617.

(9) Venkataramana, G.; Sankararaman, S. *Org. Lett.* **2006**, *8*, 2739.

(10) Jiang, W.; Fu, Q.; Fan, H.; Ho, J.; Wang, W. *Angew. Chem., Int. Ed.* **2007**, *46*, 8445.

(11) Bouffard, J.; Kim, Y.; Swager, T. M.; Weissleder, R.; Hilderbrand, S. A. *Org. Lett.* **2008**, *10*, 37.

(12) Shibata, A.; Furukawa, K.; Abe, H.; Tsuneda, S.; Ito, Y. *Bioorg. Med. Chem. Lett.* **2008**, *18*, 2246.

(13) Leroy-Lhez, S.; Fages, F. *Eur. J. Org. Chem.* **2005**, *13*, 2684.

SCHEME 1. Syntheses of 1,6- and 1,8-Diethynylpyrenes 5−10 and the Thiol Probes of 11 and 12[a]

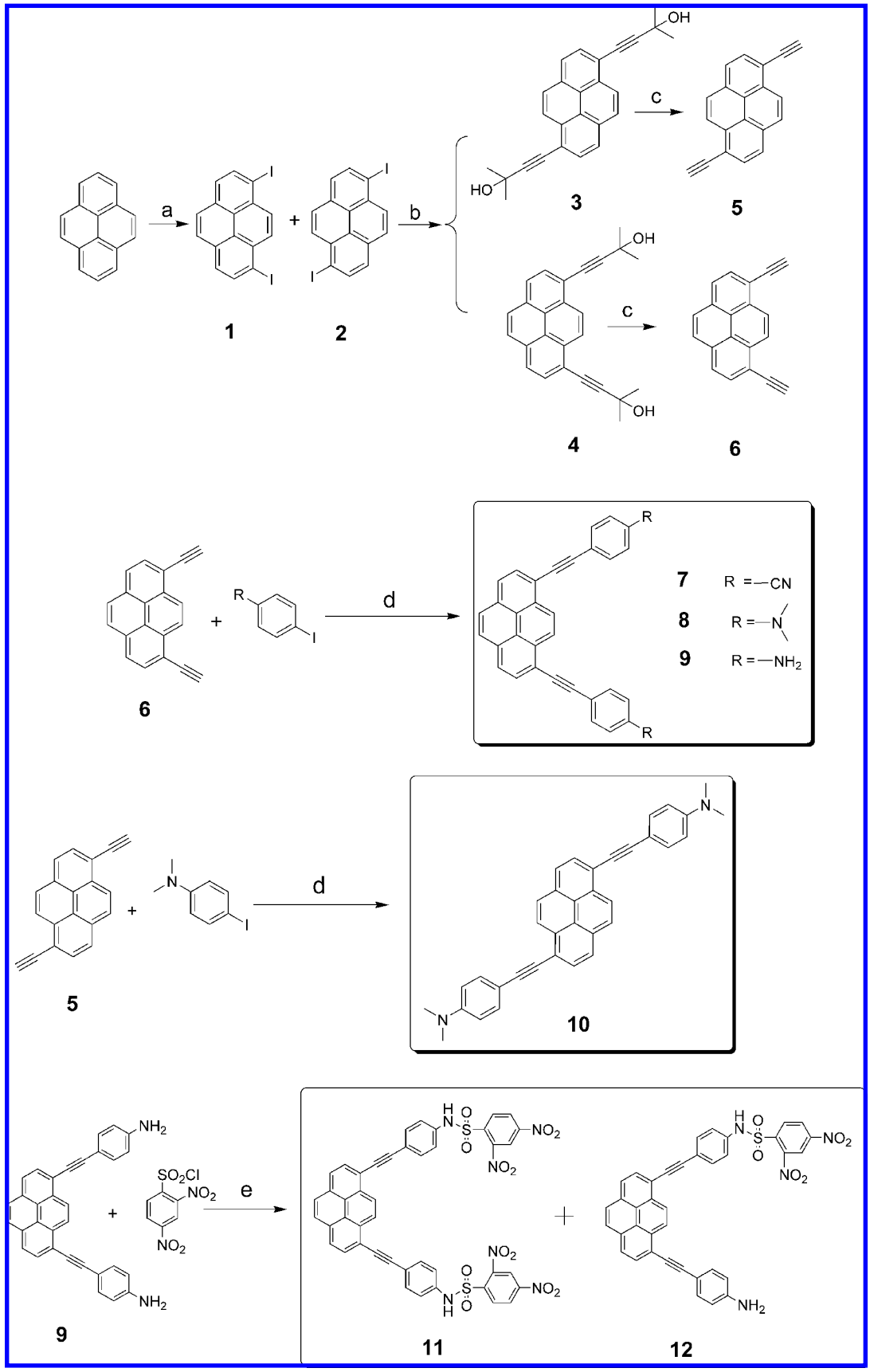

[a] (a) I_2/KIO_3(1.0/0.4 equiv), $CH_3COOH/H_2O/H_2SO_4$ (100/10/1, V/V), 40 °C, 4 h. 22%. (b) 2-Mehyl-but-3-yn-2-ol (2.3 equiv), Et_2NH, $Pd(PPh_3)_2Cl_2$ (2.3% mol), CuI (2.7% mol), Ar, 50 °C, 20 h. (c) NaOH (9 equiv), toluene, reflux, 4 h, 40%. (d) NEt_3-THF, $Pd(PPh_3)_2Cl_2$ (2% mol), CuI (4% mol), PPh_3 (4% mol) Ar, 50 °C. 4 h. (e) Anhydrous CH_2Cl_2, 2,4-dinitrobenzenesulfonylchloride (2.4 equiv), 2,6-lutidine (3.0 equiv), r.t., 45 h.

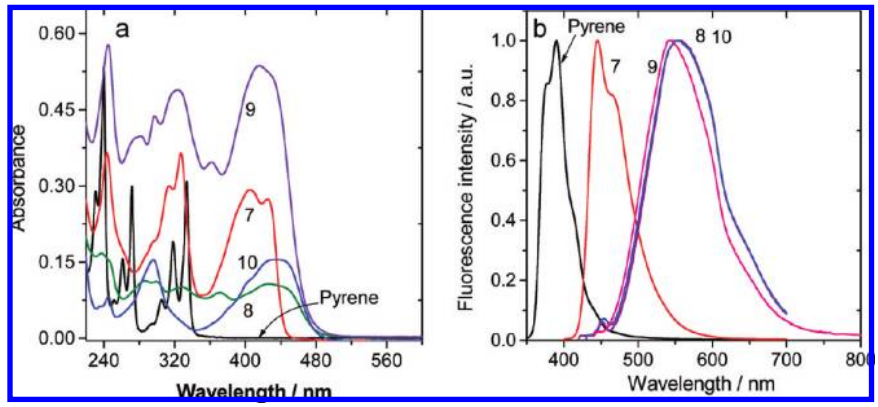

FIGURE 1. (a) UV−vis absorption spectra and (b) normalized fluorescence emission spectra of dyes **7**, **8**, **9** and **10**; 1.0×10^{-5} mol dm^{-3} of dyes in methanol. The UV−vis absorption and emission of pyrene are included for comparison.

(DMP) as the catalyst. The bis-protected and the monoprotected fluorophore, that is, probes **11** and **12** were obtained and both were studied for detection of thiol, either for in vitro detection or in vivo fluorescence imaging of thiols in living cells and different sensing property were found for probe **11** and **12**.

UV−Vis Absorption: The Effect of ICT. The absorption spectra of the pyrene derivatives in methanol are presented in Figure 1a. The ethynylpyrenes show 80 nm of red-shifted absorption compared to pyrene (320 nm). For **7**, a derivative with −CN appendent, a structured absorption band centered at 410 nm was observed. For **8**, **9** and **10**, however, the intense absorption bands at about 400 nm are lack of vibronic structure.[3] The intense and red-shifted absorption at 400 nm indicates that there is strong electronic coupling between the appended arylethynyl unit and the pyrene core, that is, efficient π-conjugation and ICT effects exist for the pyrene derivatives.[5] We propose that the structureless absorption bands are due to the significant ICT character of the fluorophore (pyrene as electron acceptor), conversely the structured absorption of **7** indicates the lack of profound ICT effect.[5] Isomers with 1,6- and 1,8-disubstitution profiles give different UV−vis absorptions, demonstrated by **8** and **10**. Furthermore, the ethynylpyrenes shows higher molar extinction coefficients (ε) than the parent pyrene, together with the larger Stokes shifts, make these derivatives ideal fluorophores for construction of molecular probes. The UV−vis absorption of the dyes in different solvents were studied and only minor solvatochromic shifts were found (see Supporting Information). The photophysical data of the ethynylpyrenes were listed in Table 1.

Fluorescence Emission Spectra: The Effect of ICT on the Solvatochromism Effect. The emission of the compounds in methanol are presented in Figure 1b. The emission of ethynylpyrene derivatives with electron pushing group is centered at 560 nm (dye **8**, **9** and **10**). Compared to pyrene, these arylethynylpyrenes show about 100 to 200 nm of red-shifted emission. Emission at longer wavelength is beneficial for fluorescent analysis, especially fluorescence bioimaging. For the derivative with electron withdrawing group (dye **7**), however, the emission is centered at 450 nm, and the vibronic structure of the pyrene emission is maintained. We noticed a monosubstituted ethynyl pyrene, which is an analogue of **8** or **10**, gives emission at 540 nm.[5] An ethynyl pyrene with similar π-conjugation framework to compound **10**, but without the dimethylamino substituent, shows emission band centered at 423 nm.[6] The emission of compound **10** (centered at 560 nm) demonstrate that electron donating group can induce substantially red-shifted emission for the ethynylated pyrene dyes.

TABLE 1. Photophysical Properties of Alkynyl-Conjugated Pyrene Derivatives 7−12 in Different Solvents

dyes	solvents	λ_{abs} (/nm)[a]	λ_{em} (/nm)[b]	$\Delta\nu$ (cm^{-1})[c]	ε (M^{-1} cm^{-1})[d]	Φ[e]
7	hexane	329/412	434/461	1230	57498	0.80
	DCM	332/412	447/474	1900	63936	0.73
	MeOH	327/405	443/469	2118	58500	0.73
8	hexane	327/421	457/485	1871	22224	0.63
	DCM	429	530	4442	21430	0.53
	MeOH	427	560	5562	21338	0.26
9	hexane	329/402	441/469	2200	93928	0.47
	DCM	331/417	480	3147	110848	0.65
	MeOH	415	551	5948	107266	0.20
10	hexane	421	456/485	1823	33830	0.69
	DCM	439	530	3911	34681	0.53
	MeOH	436	559	5047	31021	0.37
11	MeOH	402	539	6323	13145	0.003
12	MeOH	406	552	6515	25144	0.016

[a] λ_{abs}: absorption wavelength (wavelength of first absorption maximum). [b] λ_{em}: emission wavelength (at the maximum intensity). [c] $\Delta\nu$: Stokes shifts. [d] ε, extinction coefficient. [e] Φ: fluorescence quantum yields, with quinine sulfate as the standard ($\Phi = 0.54$ in 0.5 M H_2SO_4).

Dyes **8**, **9** and **10**, all appended with electron pushing group, are characterized with broad emission bands, inferring the ICT feature of the lowest-lying excited state.[3,5] For **7**, in which an electron withdrawing group (−CN) is appended, however, structured emission was observed (Figure 1b). The fluorescence quantum yield of **7** is high and is independent of solvent polarity (Table 1). For **8**, **9** and **10**, however, the fluorescence quantum yields are lower in polar solvents than that in nonpolar solvents. These results infer that ICT occurs for **8**, **9** and **10** (with pyrene unit as the electron acceptor), but not for **7**.[5] The fluorescence quantum yields of the designed thiol probe **11** and **12** are very low (predicted by DFT/TDDFT calculations, which were carried out prior to the synthesis of the probes, will be discussed later). Different from pyrene, no excimer emissions were observed for these arylethynylpyrenes, which may be due to the lack of stable $\pi-\pi$ stacking effect. The increased molar extinction coefficients and the bathochromic excitation/emission (shifts up to about 100 and 200 nm, respectively) are beneficial for the application of these dyes for fluorescence analysis, for example, in vivo fluorescent bioimaging.

The ICT effect can be better understood by performing solvatochromic studies for all compounds in solvents with different polarity.[5] The emission spectra of the dyes, especially for those with electron pushing groups (e.g., **8**, **9** and **10**), are strongly dependent on solvent polarity (Figure 2b), which is

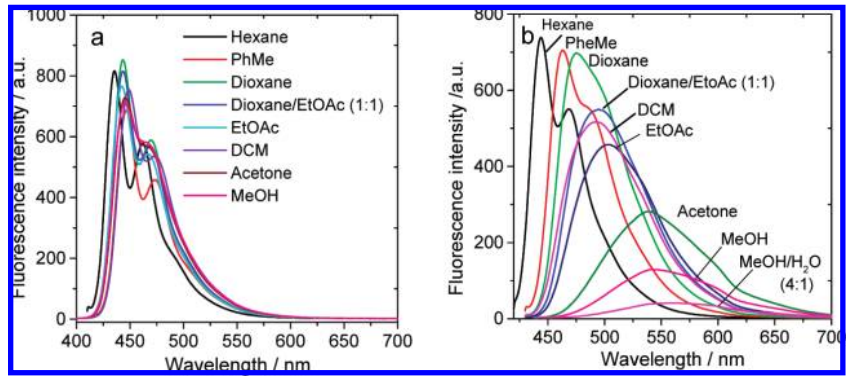

FIGURE 2. Selected emission spectra of ethynyl-conjugated pyrene derivatives (a) dye **7** and (b) dye **9** (1.0×10^{-5} mol dm^{-3}) in different solvents. In order to demonstrate the relative fluorescence intensity of the dyes in different solvents, the emission spectra were not normalized.

due to the general solvent polarity effect (see Supporting Information).[1a,b,14] On the contrary, the emission of **7** is independent of solvent polarity and the vibronic structure of the emission of pyrene is maintained (Figure 2a). We noticed a monosubstituted ethynyl pyrene with electron withdrawing substituent, however, shows structureless emission band.[5]

We carried out DFT and TDDFT calculations for these arylethynylpyrenes to investigate the relation between the polarity-dependent emission and the ICT feature of the dyes (see Supporting Information). The geometry of these molecules are coplanar according to the optimization result, which is supported by the intense UV−vis absorption at 400 nm, this 100 nm of red-shifted absorption indicates efficient electronic communication between the pyrene core and the peripheral appendents.[5] The emissive state of **7** is basically a locally excited (LE) state as suggested by the HOMO−LUMO distributions. For **9**, however, the emissive state is characterized with more significant electron redistribution, i.e. ICT feature. Similar results were found for **8** and **10** (see Supporting Information). The calculated excitation energy for the transition of $S_1 \leftarrow S_0$ of **7** and **9** are 473 and 472 nm (in vacuum), respectively. These values are close to the experimental result of 412 and 402 nm (absorption in hexane). These calculations rationalized the explanation of ICT origin of the solvent polarity dependency of the dyes' emission (Figure 2).

The ICT feature of the emission of the dyes was also demonstrated by the emission-pH profile of **9** (Figure 3). At neutral and basic pH, the fluorescence was characterized with ICT emission, that is, broad and structureless emission band centered at 560 nm. Protonation of the amino group will inhibit the formation of the ICT state, but generate the LE state, which eventually leads to a blue-shifted emission.[15] By decreasing the pH of the solution, that is, with protonation of the N atom, the emission intensity at 560 nm decreased and a new structured emission band at 420 nm developed (Figure 3). This spectral change upon pH variation is in full agreement with the proposed ICT mechanism. The emissive state at neutral and basic pH range (free amine) is in ICT feature, but at acidic pH (the amino unit is protonated), the ICT emissive state is not accessible and the emissive state is basically in LE feature. These results infer that pyrene unit is slightly electron deficient. This finding is important for future design of new pyrene-based fluorophores. No isosbestic point was observed and two different pK_a values can be derived from the titration (Figure 3, apparent pK_a^1 and pK_a^2). These observations may be due to the fact that more than two species were involved in the equilibrium, for example, the free dye **9**, the monoprotonated dye **9** and the bis-protonated dye **9**. We propose the first p$K_a^1 = 3.00$ is due to the first step of the protonation of the dye **9** ($[9\text{-H}]^+$ as the product) and the second p$K_a^2 = 1.70$ is due to the second step of the protonation ($[9\text{-H}_2]^{2+}$ as the product).

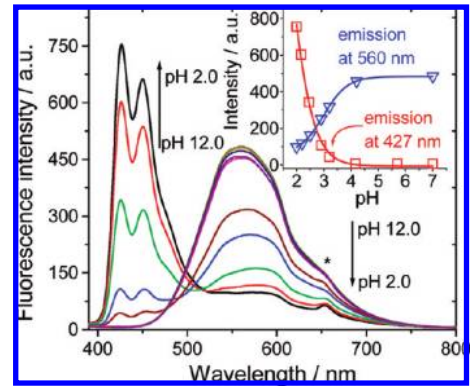

FIGURE 3. pH-dependency of the fluorescence emission of **9**. $\lambda_{ex} =$ 334 nm, 1.0×10^{-5} mol dm^{-3} of **9** in MeOH-H_2O (4/1, V/V). Apparent p$K_a^1 = 3.00 \pm 0.01$ ($r^2 = 0.99$) by emission at 560 nm, p$K_a^2 = 1.70 \pm 0.12$ ($r^2 = 0.99$) by emission at 427 nm. (Inset) Emission intensity at 427 and 560 nm vs the pH of the solution, the solid lines are the fitting results. *The minor emission shoulder at 668 nm is due to the second-order transmission of the spectrophotometer's monochromator.

As the emission of the dyes are strongly dependent on solvent polarity (Figure 2b), the solvent effect of the dyes were studied in detail with the Lippert−Mataga plots (eq 1).[1a,14] Lippert−Mataga plots can be used to evaluate the dipole moment changes of the dyes with photoexcitation, and to clarify the solvent effect as a general polarity effect or a specific solvent effect, such as hydrogen bonding.[1a,b] Linear Lippert−Mataga plot infers general solvent effect, conversely curves with upward or downward curvature infer specific solvent effect, such as hydrogen bonding between the solvent molecules and the dye molecules.[1a,14] A specific solvent effect, for example, hydrogen bond, can possibly quench the fluorescence.[1a,14,16]

$$\Delta\nu = \frac{2\Delta f}{4\pi\varepsilon_0 \hbar c a^3}(\mu_e - \mu_g)^2 + b \qquad (1)$$

(14) Han, F.; Chi, L.; Wu, W.; Liang, X.; Fu, M.; Zhao, J. *J. Photochem. Photobio. A: Chem.* **2008**, *196*, 10.

$$\Delta f = \frac{\varepsilon - 1}{2\varepsilon + 1} - \frac{n^2 - 1}{2n^2 + 1}$$

where $\Delta\nu = \nu_{abs} - \nu_{em}$ stands for Stokes shift, ν_{abs} and ν_{em} are absorption and emission (cm^{-1}), $\hbar$ is the Planck's constant, c is the velocity of light in vacuum, a is the radius of the solvent cavity in which the fluorophore resides (Onsager cavity radius) and b is a constant. Δf is the orientation polarizability, μ_e and μ_g is the ground-state dipole in the ground-state geometry and the excited dipole in the excited-state geometry and ϵ_0 is the permittivity of the vacuum. $(\mu_e - \mu_g)^2$ is proportional to the slope of the Lippert−Mataga plot.

Lippert−Mataga plots were constructed for **7** and **9** (Figure 4) and linear curves were observed, infers that no specific solvent effect exist.[1a,14] To secure this postulation, we carried out fluorescent MeOH titration of the PhMe solution of the **9**.[14] Linear plot, instead of a curve with burst phase (i.e., a sharp change at the beginning of the titration) was observed (Figure 4). This linear plot unambiguously demonstrated that the quenching effect of the alcohols on the emission of **9** (see Supporting Information) is mainly due to the general solvent effect.[1a,14] **8** and **10** show similar solvent sensitivity, which means the regioisomers do not show different photophysical properties.

The Lippert−Mataga plot of **7** gave much smaller slop than the other dyes (Figure 4 and Supporting Information), which infers smaller dipole moment changes for **7** with photoexcitation.[1a,14] The dipole moment changes of the dyes **7**, **8**, **9** and **10** were calculated as 11.9 D, 31.7 D, 35.7 and 34.8 D, respectively (eq 1). These large values may be due to the size of the molecules and the efficient charge separation.[1a,b]

Dark Lowest-Lying Excited State Induced by ICT Effect: Theoretical Calculation Aided Design of Fluorescent Thiol Probes 11 and 12. Changes in the levels of cellular thiols are closely related to clinical abnormalities, thus, fluorescent molecular probes for detection of thiol compounds is of great interest.[10,17−19] For these fluorescent thiol probes, usually the fluorophores bear electrophilic groups (e.g., iodoacetamides and benzyl halides), to which thiols may be covalently attached via electrophilic substitution. Alternatively fluorophore attached with maleimides unit are used as thiol probes.[1a,18] Fluorophores containing −CHO group are also popular for construction of thiol probes, which are based on ICT effect. In this kind of probes, -CHO group, usually as the electron acceptor of the ICT, can be transformed to thiazolidine, which is electron-donating. Thus ratiometric as well as fluorescent OFF−ON signal transduction were observed for these ICT based probes in the presence of cysteine.[19] Recently, fluorophores protected by 2,4-dinitrobenzenesulfonyl ester have been reported as new thiol sensing mechanism.[10−12] These new thiol probes inspired us to prepared pyrene based thiol probe and to investigate the sensing mechanism from a point of view of quantum chemistry.

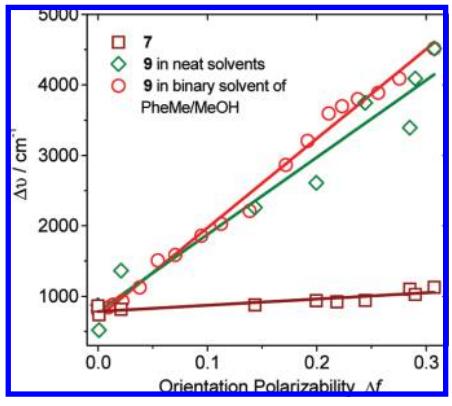

FIGURE 4. Lippert−Mataga regressions of the dyes **7** and **9**. Stokes shifts (cm^{-1}) vs the Lippert solvent parameters of orientation polarizability (Δf). For the solvents used, see experimental section. The change of the Stokes shift of **9** in binary solvent (PheMe/MeOH, with increasing MeOH) is also included. Solid lines are the fitting result with the Lippert−Mataga equation (eq 1). **7**, $r^2 = 0.80$; **9**, in neat solvents $r^2 = 0.95$, in binary solvents $r^2 = 0.99$.

Herein we designed new fluorescent thiol probes with the 2,4-dinitrobenzenesulfonyl motif.[10−12] We wish to clarify several questions with the design of the probes. First, we wish to reveal the new sensing mechanism of these thiol sensor from a point of view of quantum chemistry, which will be helpful for future probe design. Second, we wish to extend the emission wavelength of the thiol probes based on ethynylpyrene. Recently a phenylethynyl pyrene based thiol probe was reported and show emission at 420 nm (with maleimide−thiol sensing motif), which is not an ideal candidate to be used for in vivo fluorescence imaging of thiols in living cells, due to the short emission wavelength.[6]

We designed thiol probe **11** and **12** with 1,8-diaminophenylethynyl pyrene **9** as the fluorophore (Scheme 1 and Figure 5). We envision that **11** and **12** will show low background emission but intensified emission in the presence of thiols, due to the cleavage of 2,4-dinitrosulfonyl group from the fluorophore by thiols, such as cysteine (Figure 5).[10−12] Herein with theoretical calculations, we will clarify what is responsible for the fluorescence OFF−ON switching effect, it is the quenching effect of the 2,4-dinitrobenzenesulfonyl unit, or the re-establishment of the D-π-A feature of the free fluorophore. The elucidation of the sensing mechanism will be helpful for selection of proper fluorophore for future design of molecular probes.

First we examined the possibility of **11** and **12** (with **9** as the fluorophore) to be used as thiol probes. The main purpose of the quantum calculation is to examine the lowest-lying singlet excited state, which is responsible for the emissive property of the probes. Higher electronic excited states are usually not directly involved in the emission of excited fluorophores, according to Kasha's rule.[1a−c,16] The critical issue is to prove the free probe is nonfluorescent but the deprotected probe is fluorescent (Figure 5). The quantum calculation of the designed probes **11**, **12** and the free fluorophore **9** were summarized in Figure 5 and Table 2. The emissive property (as well as the excitation) of a dye can be evaluated by the quantum mechanics selection rule, e.g. the symmetry and the overlapping of the molecular orbitals (MOs), the change of the spin state and the oscillator strength (f) of the electronic transitions, etc.[1a−c,16] The calculated excitation energy for the transition of $S_1 \leftarrow S_0$ of **9** is 472 nm (in vacuum), which is close to the experimental result of 402 nm (absorption in hexane). This $S_1 \leftarrow S_0$ transition is a fully allowed transition, indicated by the overlapping of the HOMO and LUMO, as well as the transition oscillator strength (f) of 0.9776.[1b,c] This means the reverse transition, that is, $S_1 \rightarrow S_0$ transition is also fully allowed, thus this dye is potentially fluorescent.[1b,c,16] For probe **11**, however, the $S_1 \leftarrow S_0$ transition is excited at much longer wavelength of 852 nm (1.45 eV), with f value of 0.0086. This small f value and the lack of overlapping for the HOMO and LUMO (Figure 5) indicates that transition from ground state to the lowest-lying excited state

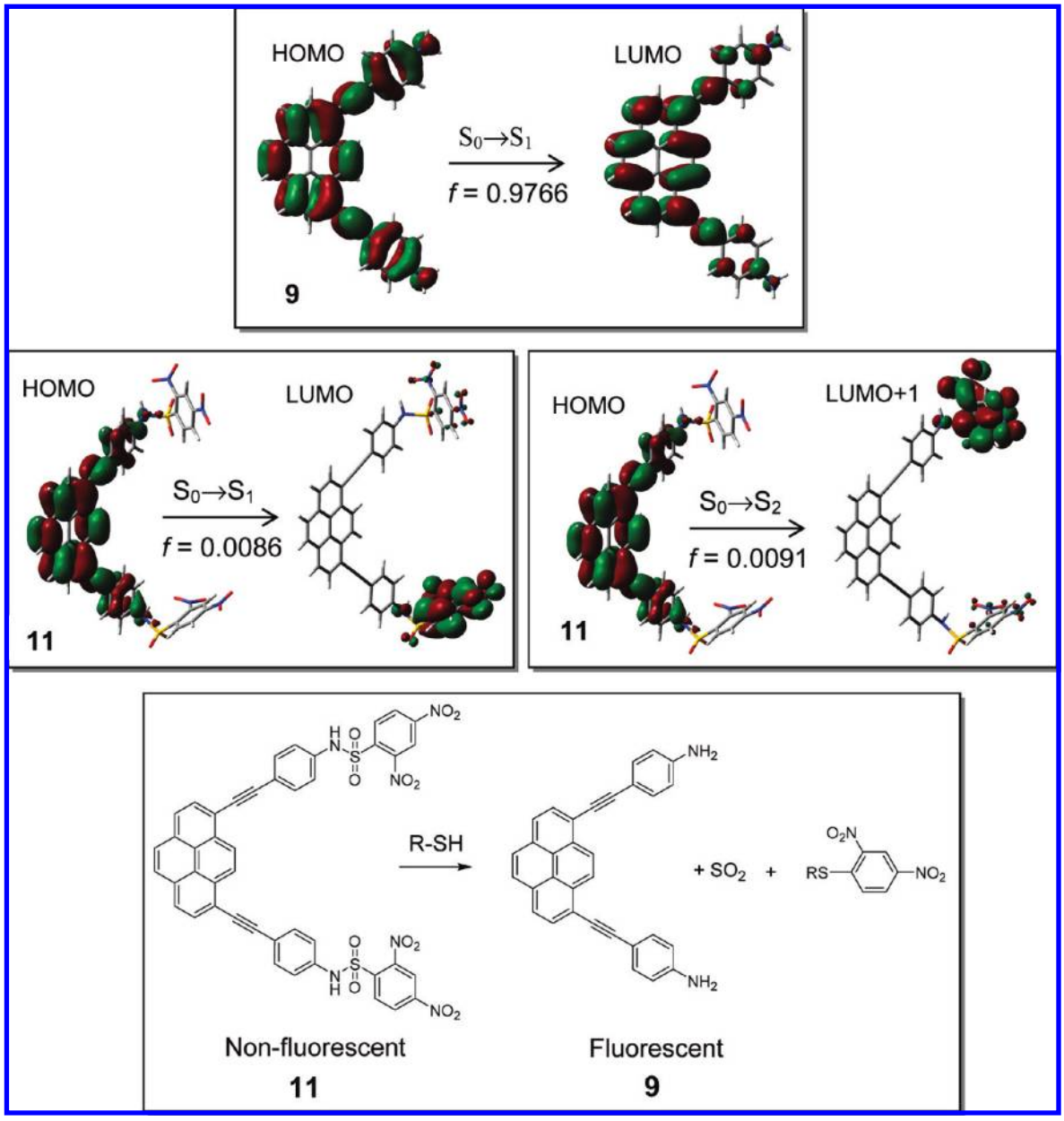

FIGURE 5. Design of thiol probes with predetermined photophysical properties. Theoretical prediction of the fluorescence OFF−ON switching effect of the designed thiol probes **11** in the presence of thiol. HOMO and LUMO of **11** and the free fluorophore **9** are presented. Note the S_1 and S_2 states of the probe **11** are isoenergetic dark states. Calculated with DFT/TDDFT at the B3LYP/6-31G(d) level using Gaussian 03.

is strongly forbidden, i.e. S_1 state is not directly accessible with photoexcitation, instead it can only be populated with inner conversion (IC) of the higher excited states, such as the allowed excited state of S_7 ($f = 1.0289$, Table 2).[1a−c] An isoenergetic electronic transition of $S_2 \leftarrow S_0$ (847 nm, 1.46 eV) was found (Table 2). This degenerated low-lying excited states S_1 and S_2 are reasonable because the ET to both the 2,4-dinitrobenzenesulfonyl units is featured with equal opportunity. The low-lying allowed transition for **11** is $S_7 \leftarrow S_0$ (464 nm). According to the Kasha's rule, the IC process is fast and S_7 will relaxes to S_1 before any possible relaxation to S_0 state.[1a−c] However, the lowest-lying excited state S_1 is dark state, i.e. nonemissive state, no radiative decay to the ground state S_0 will occur (in this case a nonradiative deactivation channel will act as a drain pipe for the excited state energy). Similar dark states of S_1 and S_2 are found for **12** (Table 2). This means dye **11** and **12** are not fluorescent. Inspection of the HOMO−LUMO (Figure 5) of **11** and **12** indicate that the dark state is due to the ICT effect, with the pyrene core as the electron donor and the 2,4-dinitrobenzenesulfonyl unit as the electron acceptor.

We demonstrated that a reported fluorescent thiol probe with similar sensing mechanism and fluorescence OFF−ON effect can be fully rationalized by the above theoretical considerations (see Supporting Information for detail).[11]

To interpret the quantum calculations in a more intuitive manner, the possible fluorescence lifetimes of dye **9**, probe **11**

(15) Zhao, G.-J.; Chen, R.-K.; Sun, M.-T.; Liu, J.-Y.; Li, G.-Y.; Gao, Y.-L.; Han, K.-L.; Yang, X.-C.; Sun, L. *Chem.—Eur. J.* **2008**, *14*, 6935.
(16) Zhao, G.-J.; Liu, J.-Y.; Zhou, L.-C.; Han, K.-L. *J. Phys. Chem. B* **2007**, *111*, 8940.
(17) Fujikawa, Y.; Urano, Y.; Komatsu, T.; Hanaoka, K.; Kojima, H.; Terai, T.; Inoue, H.; Nagano, T. *J. Am. Chem. Soc.* **2008**, *130*, 14533.
(18) (a) Matsumoto, T.; Urano, Y.; Shoda, T.; Kojima, H.; Nagano, T. *Org. Lett.* **2007**, *9*, 3375. (b) Weh, J.; Duerkop, A.; Wolfbeis, O. S. *ChemBioChem* **2007**, *8*, 122.

TABLE 2. Selected Electronic Excitation Energies (eV) and Corresponding Oscillator Strengths (*f*), Main Configurations and CI Coefficients of the Low-lying Electronically Excited States of 9, 11 and 12[a]

dyes	electronic transitions	TDDFT//B3LYP/6-31G(d) energy (eV)[b]	f[c]	composition[d]	CI[e]
9	$S_0 \rightarrow S_1$	2.63 eV (472 nm)	0.9776	HOMO→LUMO	0.6411
	$S_0 \rightarrow S_2$	3.05 eV (406 nm)	0.1048	HOMO−1→LUMO	0.6072
				HOMO→LUMO+1	0.3417
	$S_0 \rightarrow S_3$	3.47 eV (357 nm)	0.5213	HOMO−3→LUMO	0.3127
				HOMO→LUMO+1	0.4722
	$S_0 \rightarrow S_5$	3.83 eV (324 nm)	0.5976	HOMO−3→LUMO	0.3780
				HOMO→LUMO+1	0.3320
				HOMO→LUMO+2	0.4262
11	$S_0 \rightarrow S_1$	1.45 eV (853 nm)	0.0086	HOMO→LUMO	0.7030
	$S_0 \rightarrow S_2$	1.46 eV (847 nm)	0.0091	HOMO→LUMO+1	0.7027
	$S_0 \rightarrow S_7$	2.67 eV (464 nm)	1.0289	HOMO→LUMO+4	0.6221
	$S_0 \rightarrow S_{25}$	3.60 eV (344 nm)	1.1588	HOMO−1→LUMO+4	0.3814
				HOMO→LUMO+7	0.4602
12	$S_0 \rightarrow S_1$	1.13 eV (1090 nm)	0.0065	HOMO→LUMO	0.7038
	$S_0 \rightarrow S_2$	1.60 eV (774 nm)	0.0004	HOMO→LUMO+1	0.7045
	$S_0 \rightarrow S_6$	2.56 eV (484 nm)	0.8528	HOMO→LUMO+2	0.6406
	$S_0 \rightarrow S_{16}$	3.41 eV (364 nm)	0.5139	HOMO−1→LUMO+2	0.3294
				HOMO→LUMO+4	0.4713

[a] Calculated by TDDFT//B3LYP/6-31G(d), based on the DFT//B3LYP/6-31G(d) optimized ground state geometries. [b] Only the low-lying excited states and some allowed transions were presented. [c] Oscillator strength. [d] Only the main configurations with configuration interaction (CI) coefficients >0.3 are presented. [e] CI coefficients are in absolute values.

and probe **12** were calculated based on the calculated data (Table 2) by using Einstein transition probabilities of the spontaneous transitions, which is described by the eq 2.[20]

$$\tau = \frac{c^3}{2 \cdot (E)^2 \cdot f} \qquad (2)$$

where τ is the fluorescence lifetime, c stands for the light velocity, E is the transition energy and f is the oscillator strength. All the parameters are in atomic unit (au). The f and E values are based on the DFT/TDDFT calculation results (Table 2). The calculated fluorescence lifetimes for dye **9**, probe **11** and probe **12** are 3.4 ns, 1270 and 2775 ns, respectively. The reasonable predicted lifetime of dye **9** infers that it may be fluorescent.[1a−c] For probe **11** and **12**, however, the exceptionally long lifetimes are far beyond the allowed lifetime range for the relaxation of a singlet excited state (usually singlet excited state is the emissive state of most organic fluorophores, with lifetimes shorter than 10 ns). These results show that probe **11** and **12** are nonfluorescent. It should be pointed out that this is a approximation because the excitation energy is used in the calculation, not the energy corresponding to the emission (optimization of the excited states are required).

Thus 2,4-dinitrophenylsulfonyl substituent quenches the fluorescence but thiols hydrolyses the phenylsulfonyl amide bond, i.e. reaction of **11** and **12** with thiol leads to dye **9** (Figure 5),[11,12] correspondingly the dark state of probe is replaced by emissive state, thus a fluorescence OFF−ON response is predicted for probes **11** and **12** in the presence of thiols.[11,16] This finding is of great interest because it relieve the restriction on using D-π-A type of fluorophore to construct this kind of thiol probes,[11] as it is known that D-π-A fluorophores usually show low fluorescence quantum yields in high polarity solvents, such as aqueous solution. Our findings offers more diversity for the selection of fluorophores in molecular probe design.

Synthesis of 11 and 12 as ICT Modulated Fluorescent Thiol Probes. Inspired by the theoretical calculations which predicts the fluorescence OFF−ON switch property of the designed thiol probes, we prepared the two probes **11** and **12** and the absorption/emission spectra with and without thiol (e.g., L-cysteine) were recorded (Figure 6).

The maximal absorption of **11** is located at ca. 400 nm. The calculated excitation energy (464 nm, $S_7 \leftarrow S_0$) is close to the experimental result.[20] The UV−vis absorption did not change significantly in the presence of thiol (Figure 6a), inferring that the D-π-A feature of the fluorophore **9** does not change profoundly with cleavage of the 2,4-dinitrobenzenesulfonyl unit. This UV−vis absorption profile is in contrast to a reported thiol probe with similar sensing mechanism,[11] and suggests that the fluorescence OFF−ON switching effect is not due to the intrinsic ICT feature of the fluorophore, instead, the 2,4-dinitrobenzenesulfonyl unit is essential.

Theoretical calculations predict a dark state S_1 for **11**. Experimentally, **11** is nonfluorescent (Figure 6b). In the presence of thiol compound, e.g. L-cysteine, however, the fluorescence is switched ON, which is in full agreement with the theoretically predicted emissive **9** (Figure 6b). The fluorescence intensity of **11** is enhanced by 53 folds. We propose the emission in the presence of cysteine is due to the deprotected amine, that is, **9** (Figure 5).[10−12] This is demonstrated by the emission spectra of **9** under similar conditions.

For the monoprotected **12**, similar fluorescence OFF−ON switch is observed. In the presence of L-cysteine, 26-folds of fluorescence intensifying is observed (see Supporting Information). This lower enhancement may be due to the lower ET efficiency for this monoprotected probe.

The reaction kinetics of probe **11** and **12** with cysteine were also investigated and the result show that the reaction is fast at room temperature and finished within 5 min (inset of Figure 6b). The reaction of probe **11** is slightly faster than that of probe **12**. We propose that dinitrophenylsulfonylamide deprotection is likely to proceed via a two-step mechanism: **11** → **12** → **9**, the slow one is assumed to be the second step.

We noticed phenylethynylpyrene has been used for fluorescent thiol probes, based on the maleimide approach.[6] However, the emission wavelength of that reported probe (centered at about 400 nm) is shorter than the probes **11** and **12** described herein (emission centered at 560 nm). The blue-shifted emission of the reported probe is probably due to the electron withdrawing effect of the maleimide group.[5,6]

As the alkynylpyrene show much shorter luminescence lifetime than pyrene, any possible interference from oxygen on the fluorescence can be eliminated.[5,6] Our experiments show the fluorescence pyrene can be profoundly quenched by oxygen (with $I_0/I_{100} = 64.1$, where I_0 is the emission intensity in deaerated solution, I_{100} is the emission intensity in oxygen saturated solution, see Supporting Information). But the fluo-

(19) (a) Lin, W.; Long, L.; Yuan, L.; Cao, Z.; Chen, B.; Tan, W. *Org. Lett.* **2008**, *10*, 5577. (b) Toutchkine, A.; Nalbant, P.; Hahn, K. M. *Bioconjugate Chem.* **2002**, *13*, 387. (c) Tang, B.; Xing, Y.; Li, P.; Zhang, N.; Yu, F.; Yang, G. *J. Am. Chem. Soc.* **2007**, *129*, 11666. (d) Tanaka, F.; Mase, N.; Barbas, C. F., III *Chem. Commun.* **2004**, 1762. (e) Zhang, D.; Zhang, M.; Liu, Z.; Yu, M.; Li, F.; Yi, T.; Huang, C. *Tetrahedron Lett.* **2006**, *47*, 7093. (f) Kim, T.-K.; Lee, D.-N.; Kim, H.-J. *Tetrahedron Lett.* **2008**, *49*, 4879. (g) Duan, L.; Xu, Y.; Qian, X.; Wang, F.; Liu, J.; Cheng, T. *Tetrahedron Lett.* **2008**, *49*, 6624. (h) Lee, K.-S.; Kim, T.-K.; Lee, J. H.; Kim, H.-J.; Hong, J.-I. *Chem. Commun.* **2008**, 6173. (i) Zhang, X.; Ren, X.; Xu, Q.-H.; Loh, K. P.; Chen, Z.-K. *Org. Lett.* **2009**, *11*, 1257.

(20) (a) Yang, L.; Ren, A.-M.; Feng, J.-K.; Wang, J.-F. *J. Org. Chem.* **2005**, *70*, 3009. (b) Liu, Y.-L.; Feng, J.-K.; Ren, A.-M. *J. Phys. Chem. A* **2008**, *112*, 3157.

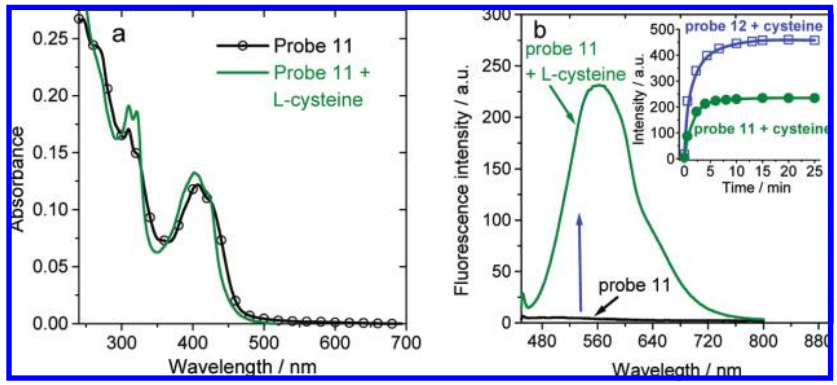

FIGURE 6. (a) UV−vis absorption and (b) fluorescence emission spectra (λ_{ex} = 441 nm) of probe **11** (1.0×10^{-5} mol dm^{-3}) before and after addition of L-cysteine in methanol/water (4/1, V/V) solution. The final concentrations of the probe and L-cysteine are 1.0×10^{-5} mol dm^{-3} and 2.0×10^{-3} mol dm^{-3}, respectively. Inset of (b): fluorescence emission intensity changes of probes **11** and **12** (1.0×10^{-5} mol dm^{-3}) as a function of elapsed time upon addition of L-cysteine (2.0×10^{-3} mol dm^{-3}) in MeOH−H_2O (4/1, V/V). λ_{ex} = 441 nm; λ_{em} = 562 nm; 25 °C.

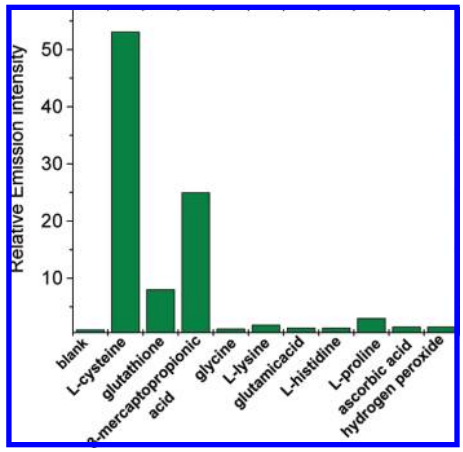

FIGURE 7. Response of probe **11** to different analytes. Relative fluorescence intensity of 10 μM probe at 562 nm (λ_{ex}= 441 nm) before and after incubation in the presence of 2 mM analytes at room temperature for 15 min. Twenty-five °C, pH 7.4, methanol/water (4/1, V/V) solution.

rescence intensity of **9** is less sensitive to oxygen (I_0/I_{100} = 1.9, see Supporting Information).

The selectivity of probe **11** for thiols over biologically relevant analytes was studied at physiological conditions (Figure 7). **11** shows a positive fluorescence response only in the presence of thiols (cysteine, reduced glutathione and 3-mercaptopropoinic acid), for which fluorescence signals were increased by 20- to 53-fold. No significant positive fluorescence response were observed in the presence of amines (lysine), reactive oxygen species (hydrogen peroxide), or reducing agents (ascorbic acid). Probe **12** shows similar thiol selectivity (see Supporting Information).

It is worth to note that the fluorescence quantum yield of **9** is 0.20 in MeOH (0.018 in MeOH−H_2O) because the fluorophore is without any profound D-π-A feature. D-π-A type of fluorophores usually show decreased emission intensity in high polar solvents, such as aqueous solution.

Fluorescence Imaging of Thiols in Living Cells. The monitoring of thiols in living pheochromocytoma cells (PC12 cells) was carried out (Figure 8). The pictures of bright field images and fluorescence images were taken by fluorescence microscope. The cells were incubated with the probes and green fluorescence was observed with **12** (Figure 8D). Weaker fluorescence image was observed with **11** (Figure 8B). We propose that **11** is less cell-permeable, possible due to its high hydrophobicity. In order to prove that the fluorescence switch on effect was due to the reaction between the probe and the intracellular thiols, we used thiol-reactive *N*-methylmaleimide to pretreat the cells to remove the intracellular thiol,[11,12] no fluorescence was observed (Figure 8, C and E). The discrepancy between the color of the bioimaging photo (Figure 8) and the emission wavelength of the dyes in solution (Table 1) is due to the different polarity of the microenvironment in which the dye molecules dwell.[1a] We also used onion epidermal cells to do the control experiment (Supporting Information). We found that **12** is onion epidermal cell-permeable but **11** is not. Yellow-green fluorescence was observed for **12** within the cell. The strong signal was localized to cytoplasm. On the other hand, nuclei showed weak fluorescence signals (see Supporting Information). In a control experiment, the onion epidermal cells were pretreated with *N*-methylmaleimide to react with the intracellular thiols. Then the onion epidermal cells were incubates with **12**, no fluorescence signal was observed. These results confirm **12** is specific for thiols over other analytes in living cells.

Conclusion

We synthesized 1,8- and 1,6-bis(phenylethynyl) pyrenes with different intramolecular charger transfer (ICT) feature and the ICT effect on the photophysical properties of these dyes were studied. For the dyes with profound ICT feature (dye **8** and **10**, appended with $-N(CH_3)_2$), broad and solvatochromic emission bands were observed. Conversely, for alkynylpyrenes with minor ICT feature (dye **7**, appended with −CN), however, solvent polarity independent and structured emission spectra were observed. Phenylethynylated pyrene derived fluorescent thiol probes with 2,4-dinitrobenzenesulfonyl amide structure were designed and were predicted by TDDFT calculations to show fluorescence OFF−ON switching effect in the presence of thiol. The TDDFT calculations predict lowest-lying dark states of S_1 for the probes, induced by ICT effect (electron transfer from fluorophore to 2,4-dinitrobenzenesulfonyl unit). This dark state infers the probe is nonfluorescent. Cleavage of the 2,4-dinitrobenzenesulfonyl unit by thiol releases the free fluorophore (the ICT effect is terminated), for which the lowest-lying excited state S_1 is no longer a dark state, therefore the product will potentially be fluorescent. These theoretical predictions on the photophysical properties of the probes were fully proved by experiments, fluorescence OFF−ON switching effect was

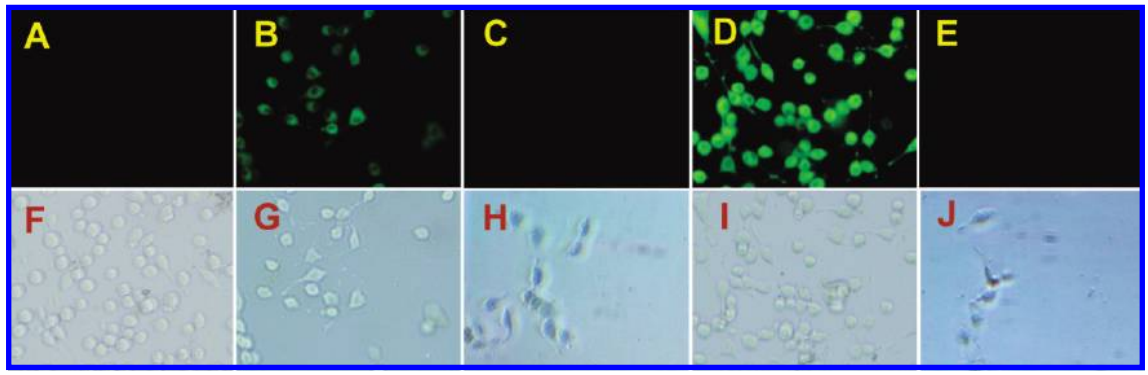

FIGURE 8. Fluorescence images of PC12 cells. (A) Fluorescence images of cell. (B) Fluorescence images of cells incubated with probe **11** (25 μM) for 20 min at 37 °C. (C) Fluorescence images of cells pretreated with *N*-methylmaleimide (0.1 mM) for 60 min at 37 °C and then incubated with probe **11** (25 μM) for 20 min at 37 °C. (D) Fluorescence images of cells incubated with probe **12** (25 μM) for 20 min at 37 °C. (E) Fluorescence image of PC12 cells pretreated with *N*-methylmaleimide (0.1 mM) for 60 min at 37 °C and then incubated with probe **12** (25 μM) for 20 min at 37 °C. (F−J) are the corresponding bright field images of (A−E).

observed for the probes **11** and **12** in the presence of thiols. The probes were successfully used for bioimaging of thiols in living cells. Our results show that the fluorescence OFF−ON switching effect of the fluorescent probe is due to the re-establishment of the emissive S_1 state of the probe, after termination of the ICT effect by cleavage of the 2,4-dinitrobenzenesulfonyl unit, instead of the recovery of the D-π-A character of the fluorophore. Our finding infers that modular fluorophore unit for this kind of thiol probes is not restricted to the D-π-A type of fluorophore, instead, dyes with diverse structure can be used for construction of fluorescent thiol probes with 2,4-dinitrobenzenesulfonyl as the thiol reactive unit. We envision that these investigation on the photophysical properties of the pyrene derived fluorophores and the successful application of DFT/TDDFT calculations in the rational design of fluorescent molecular probes are of great interest for development of new fluorophores and molecular probes with predetermined photophysical properties.

Experimental Section

Compound 7. 1-Cyano-4-iodobenzene (58.0 mg, 0.25 mmol) was dissolved in 5 mL Et_3N. The solution was purged with argon, then $Pd(PPh_3)_2Cl_2$ (3.8 mg, 5.4 μmol), PPh_3 (2.7 mg, 0.01 mmol), **6** (50.0 mg, 0.12 mmol) and CuI (1.9 mg, 0.01 mmol) were added. The reaction mixture was heated at 60 °C for 7 h. The solvent was removed under vacuum and subjected to column chromatography (silica gel, dichloromethane/petroleum ether, 2/1, V/V). Compound **7** was obtained as a orange solid (20.0 mg, yield: 35.0%). Mp 293.7−294.5 °C.^{1}H NMR (400 MHz, $CDC1_3$) δ 8.75 (s, 2H), 8.27(d, 2H, J = 12.0 Hz), 8.21(d, 2H, J = 8.0 Hz), 8.13(s, 2H), 7.81 (d, 4H, J = 7.6 Hz), 7.73 (d, 4H, J = 8.4 Hz), HRMS: *m/z* calcd for $C_{34}H_{16}N_2$ ($[M + H]^+$) 452.1313, found 452.1306.

Compounds **8** and **10** were synthesized by the same method. **8**: orange powder, yield: 40.0%. Mp 249.1−250.4 °C. ^{1}H NMR (400 MHz, $CDC1_3$) δ 8.78 (s, 2H), 8.18 (d, 2H, J = 8.0 Hz), 8.11 (d, 2H, J = 8.0 Hz), 8.03 (s, 2H) 7.64 (d, 4H, J = 8.8 Hz), 6.82 (m, 4H), 3.06 (s, 12H). HRMS: *m/z* calcd for $C_{36}H_{28}N_2$ ($[M + H]^+$) 488.2252, found 488.2252. **10**: orange powder, yield: 32.0%. Mp >300 °C. ^{1}H NMR (400 MHz, $CDC1_3$) δ 8.68 (d, 2H, J = 9.6 Hz), 8.13−8.21 (m, 6H), 7.68 (d, 4H, J = 8.0 Hz), 7.30 (m, 4H), 3.10 (s, 12H). HRMS: *m/z* calcd for $C_{36}H_{28}N_2$ ($[M + H]^+$) 488.2252, found 488.2256.

Compound 9. 4-Iodoaniline (121.5 mg, 0.56 mmol) was dissolved in 8 mL Et_3N. The solution was degassed and purged with argon, then $Pd(PPh_3)_2Cl_2$ (7.1 mg, 0.01 mmol), PPh_3 (5.3 mg, 0.02 mmol), **6** (100.0 mg, 0.25 mmol) and CuI (4.5 mg, 0.02 mmol) were added under argon. The reaction mixture was heated at 60 °C for 7 h. The solvent was removed under vacuum and the residue was subjected to column chromatography (silica gel, petroleum methanol/dichloromethane, 1/150, V/V). Compound **9** was obtained as a orange solid (90 mg, 82.0%). Mp 213.1−214.3 °C. ^{1}H NMR (400 MHz, DMSO-d_6) δ 8.75 (s, 2H), 8.17(d, 2H, J = 8.0 Hz), 8.10 (d, 2H, J = 8.0 Hz), 8.02 (s, 2H), 7.54(d, 4H, J = 8.4 Hz), 6.73(d, 4H, J = 8.4 Hz), 3.88(s, 4H), HRMS: *m/z* calcd for $C_{32}H_{20}N_2$ ($[M + H]^+$) 432.1626, found 432.1630.

Compound 11 and 12. To a stirred solution of **9** (60.0 mg, 0.14 mmol) and 2,6-lutidine (50 μL, 0.39 mmol) in anhydrous dichloromethane (10 mL) was added 2,4-dinitrobenzeneslfonyl chloride (100.0 mg, 0.34 mmol) in portions at 0 °C. The reaction mixture was allowed to stir for 45 h as it slowly warms up to room temperature. The solvent was removed under vacuum to give a mixture of **11** and **12**. The crude product was then subjected to column chromatography (silica gel, dichloromethane/methanol, 100/1, V/V). Compound **11** and **12** was obtained as yellow brown solid. The yield of **11** and **12** are 25.0 mg (20.0%) and 40.0 mg (43.0%), respectively. **11**: ^{1}H NMR (400 MHz, DMSO-d_6) δ 8.90 (s, 2H), 8.73(s, 2H), 8.61−8.63(d, 2H, J = 8.0 Hz), 8.37(d, 2H, J = 8.0 Hz), 8.25−8.30 (q, 6H, J = 8.0 Hz), 7.70 (d, 4H, J = 8.0 Hz), 7.24(d, 4H, J = 8.4 Hz). ^{13}C NMR(100 MHz, DMSO-d_6): δ 149.8, 147.8, 132.7, 131.6, 131.0, 130.9, 129.8, 128.1, 127.1, 126.2, 125.8, 123.3, 120.7, 120.2, 117.6, 95.5, 88.0, 79.1, 28.9. HRMS: *m/z* calcd for $C_{44}H_{23}N_6O_{12}$ ($[M - H]^-$) 891.0815, found 891.0836. **12**: ^{1}H NMR (400 MHz, DMSO-d_6) δ = 8.94 (s, 1H), 8.72 (d, 2H, J = 5.6 Hz), 8.62−8.65 (d, 1H, J = 6.8 Hz), 8.19−8.34 (q, 7H,), 7.75 (d, 2H, J = 8.8 Hz), 7.45 (d, 2H, J = 8.0 Hz), 7.28 (d, 2H, J = 8.4 Hz), 6.66 (d, 2H, J = 8.0 Hz), 5.75 (m, 2H). ^{13}C NMR (100 MHz, DMSO-d_6) δ 150.6, 150.4, 148.3, 136.5, 133.4, 132.1, 131.7, 131.6, 130.8, 130.7, 130.3, 129.8, 128.8, 128.1, 127.8, 127.0, 126.3, 125.9, 123.9, 121.1, 120.9, 119.6, 119.2, 117.5, 114.2, 108.5, 98.9, 95.5, 88.8, 86.0. HRMS: *m/z* calcd for $C_{36}H_{21}N_4O_6$ ($[M - H]^-$) 661.1182, found 661.1171.

UV−Vis and Fluorescence Spectra. The concentration of the dyes was fixed at 1.0×10^{-5} mol dm^{-3} for the pH titration. pH measurements were carried out with a Delta 320 Microprocessor pH meter (Mettler Toledo). The fluorescence spectra of the dyes were recorded as the pH was changed from pH 2 to 11 in approximate intervals of approximately 0.5 pH units. The pH was controlled using minimum volumes of sodium hydroxide and hydrochloric acid solutions. For the Lippert−Magata plots (Figure 4), the solvents used were hexane, toluene, dioxane, dioxane/ethyl acetate (1/1, V/V), ethyl acetate, dichloromethane, acetone, 1-hexanol, ethanol and methanol (in the order of increasing Δf values). Curves were constructed using the Origin 5.0 (Microcal software).

Theoretical Calculations. The ground state structure of the dyes and probes were optimized using density functional theory (DFT) with B3LYP functional and 6-31G (d) basis set. The excited state related calculations were carried out with the Time dependent density functional theory (TD-DFT) with the optimized structure of the ground state (DFT/6-31G(d)). There are no imaginary frequencies in frequency analysis of all calculated structures, therefore each calculated structure is an local energy minimum. All these calculations were performed with Gaussian 03.

Fluorescence Microscopy and Cell-Uptake Studies. PC12 cells were grown in DMEM (Dulbecco's Modified Eagle's Medium) in an atmosphere of 5% CO_2, 95% air at 37 °C. Cells were plated on 24-well plate and allowed to adhere for 24 h. After 24 h, the cells were washed with PBS (phosphate buffered saline) and then incubated at 37 °C in the presence probe **11** or **12** (25 μM, 0.5:100 DMSO/DPBS, V/V, pH 7) for 20 min. Fluorescence imaging was performed after washing the cells three times with PBS buffer. The fluorescence images were obtained using an OLMPUS IX-71 fluorescence microscope with blue excitation module. The exposure times for PC12 cells were 0.02 s (with 640× magnification), for onion epidermal cells, the exposure times were 0.25 s (with 160× magnification). The images for the thiol-dependent activation and corresponding maleimide controls were taken with identical settings.

Acknowledgment. We thank the NSFC (20642003 and 20634040), Ministry of Education (SRF for ROCS, SRFDP-200801410004 and NCET-08-0077), PCSIRT(IRT0711), Cultivation Fund of the Key Scientific and Technical Innovation Project (707016), State Key Laboratory of Fine Chemicals (KF0710 and KF0802), State Key Laboratory of Chemo/Biosensing and Chemometrics (2008009) and Dalian University of Technology (SFDUT07005) for financial support. We are also grateful to the reviewers for their critical and helpful comments on the manuscript.

Supporting Information Available: General experimental methods, ^{1}H and ^{13}C NMR data of the compounds, photophysical data and solvent effect of the dyes, oxygen sensitivity of the emission intensity, response of probe **12** to thiols, theoretical calculations details (including z-matrix), theoretical rationalization of the sensing mechanism of a reported thiol probe, fluorescence imaging of thiol in living cells. This material is available free of charge via the Internet at http://pubs.acs.org.

JO900588E